GEOPHYSICAL RESEARCH LETTERS, VOL. 36, L17810, doi:10.1029/2009GL039422, 2009

Does the location of aircraft nitrogen oxide emissions affect their climate impact?

David S. Stevenson[1] and Richard G. Derwent[2]

Received 2 June 2009; revised 17 July 2009; accepted 5 August 2009; published 11 September 2009.

[1] We present results from 112 one-year global chemistry-transport model integrations: a base case, then variants with extra aircraft nitrogen oxide (NO_x) emissions added to specific regions in the first month (July). The NO_x stimulates ozone (O_3) production and methane (CH_4) destruction. Responses vary spatially: low background NO_x regions are most sensitive. Integrated (100-year time horizon) radiative forcings (IRF) are calculated. Net (O_3 + CH_4) IRFs for July aviation NO_x are generally negative: the global average, weighted by emissions, is -1.9 mWm^{-2} yr (TgNO$_2$)$^{-1}$. The positive IRF associated with the short-term O_3 increase (4.1 mWm^{-2} yr (TgNO$_2$)$^{-1}$) is overwhelmed by the effects of the long-term CH_4 decrease. Aircraft NO_x net IRFs are spatially variable, with July values over the remote Pacific approximately balancing the IRF associated with aviation CO_2 emissions (28 mWm^{-2} yr (TgNO$_2$)$^{-1}$). The overall climate impact of global aviation is often represented by a simple multiplier for CO_2 emissions. These results show that this is inappropriate.
Citation: Stevenson, D. S., and R. G. Derwent (2009), Does the location of aircraft nitrogen oxide emissions affect their climate impact?, *Geophys. Res. Lett.*, *36*, L17810, doi:10.1029/2009GL039422.

1. Introduction

[2] The global fleet of aircraft currently account for 2–3% of global anthropogenic CO_2 emissions [*Lee et al.*, 2009], yet these emissions fall outside the remit of the Kyoto Protocol. Between 1970 and 2005 total anthropogenic CO_2 emissions increased by a factor of 2.0; at the same time, aviation CO_2 emissions rose considerably faster ($\times$ 2.6) [*Lee et al.*, 2009]. Aircraft emit other climatically important trace species, including oxides of nitrogen (NO_x = NO + NO_2) and sulphur, water vapour and particulate matter; they also generate contrails [*Schumann*, 2005] and perturb cirrus clouds [*Stordal et al.*, 2005]. The contribution of aircraft CO_2 towards the radiative forcing (RF) of climate change is relatively well constrained, and is independent of emission location. RFs resulting from the other processes are much less certain, and many of these are dependent on emission location. For example, J. M. Haywood et al. (A case study of the radiative forcing of persistent contrails evolving into contrail-induced cirrus, submitted to *Journal of Geophysical Research*, 2009), find a large positive localised RF over the North Sea associated with contrail-induced cirrus, however, the spatio-temporal occurrence of such cases, and their global RF, are not well known. Nevertheless, the overall contribution of aircraft to climate change is thought to be larger than that just due to the CO_2 they emit alone [*Forster et al.*, 2006; *Lee et al.*, 2009].

[3] Significant uncertainty surrounds the RF produced by aircraft NO_x emissions. NO_x promotes tropospheric ozone (O_3) production, but also stimulates methane (CH_4) destruction by generating hydroxyl radicals (OH) [*Wild et al.*, 2001; *Derwent et al.*, 2001; *Köhler et al.*, 2008]; NO_x also generates nitrate aerosol and, through changes in oxidants, affects production of other secondary aerosols. These impacts of NO_x on aerosols, and other interactions between gas-phase and aerosol chemistry are not studied here. *Stevenson et al.* [2004] (hereafter referred to as ST04) showed that the response of O_3 and CH_4 to aircraft NO_x is seasonally dependent. Here we extend that analysis to consider how important the emission location is in influencing the impact of aviation NO_x on O_3 and CH_4.

2. Model and Experiments

[4] We used the STOCHEM global Lagrangian chemistry transport model (CTM), driven by meteorological analyses for 1998 from the Met Office Unified Model. The CTM includes a 70 species tropospheric chemistry scheme and has a horizontal resolution of 5° $\times$ 5°, with nine equally spaced vertical levels extending from the surface to $\sim$100 hPa. Full details of the model version employed and the pulse methodology are given elsewhere [*Derwent et al.*, 2008]. Slightly different versions of the same model have been employed in several intercomparisons, and simulated O_3 and OH compare well with other state-of-the-art models and observations [e.g., *Stevenson et al.*, 2006].

[5] A total of 112 integrations were performed; we refer to the first as the base experiment. All integrations ran for one year beginning 1st July, with emissions appropriate for year 2000, including aircraft NO_x, as used by *Dentener et al.* [2005]. The 111 variants were all identical to the base except that aircraft NO_x emissions were increased during the first month of the integration in a particular 10° $\times$ 10° region at cruise altitude ($\sim$200–300 hPa) by 4 kg (NO_2) s^{-1}, equivalent to an extra 10 Gg (NO_2) over the month.

3. Results

[6] We analyse the different responses of CH_4 and O_3 in each experiment, relative to the base (Figure 1). In all cases, a short-lived, regionally distinct, positive O_3 anomaly is produced (Figure 1a), which decays away within a few (<4) months (Figure 1b). The extra NO_x and O_3 enhance

[1]School of GeoSciences, University of Edinburgh, Edinburgh, UK.
[2]rdscientific, Newbury, UK.

0094-8276/09/2009GL039422$05.00

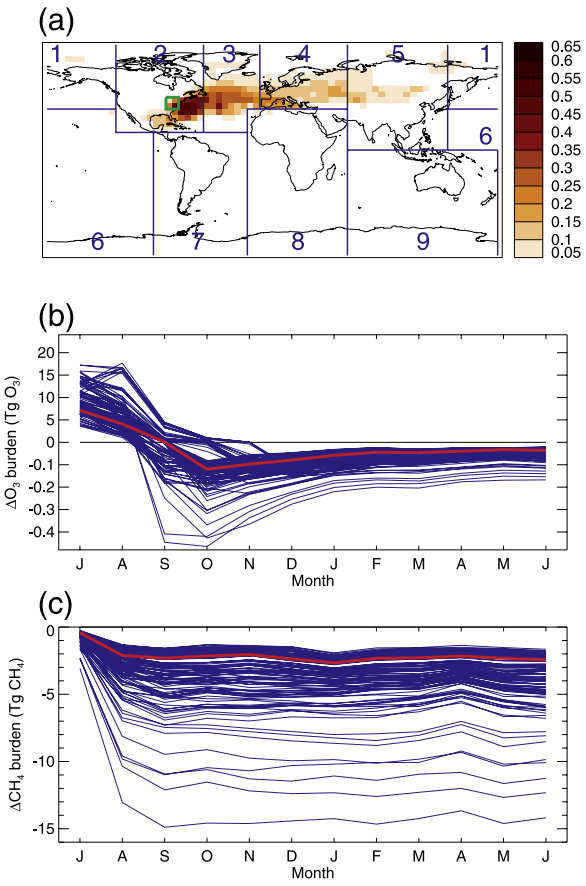

Figure 1. (a) The monthly mean change in ozone (ppb) at 250 hPa for July (the month of extra emissions), for an experiment releasing extra aircraft NO_x over eastern N. America (green box), relative to the base case. The numbered regions are referred to in Table 2. (b) Change in tropospheric ozone burden (Tg) (thick red line) for the 12 months from July. NB the negative scale has been expanded by a factor of 50 for clarity. The thin blue lines show the change for all the other experiments. (c) Same as Figure 1b but for methane. Results in Figure 1a are for the pulse magnitude used in the experiment (10 $Gg(NO_2)$), whilst Figures 1b and 1c show results normalised to a 1 $Tg(NO_2)$ pulse.

levels of OH, depleting CH_4. A negative CH_4 anomaly builds up over the first few months of each experiment, before starting to decay with the 11.5 year CH_4 perturbation lifetime (Figure 1c). As CH_4 is an O_3 precursor, the CH_4 depletion is accompanied by a small negative O_3 anomaly, which overrides the effects of the initial positive O_3 anomaly within a few months (Figure 1b). Figures 1b and 1c display the perturbations to the O_3 and CH_4 global burdens for all the experiments, illustrating that aircraft emissions from different locations produce a range of different responses.

[7] The O_3 and CH_4 anomalies from each experiment have been used to calculate time-integrated radiative forcings (RF). We integrate over a 100-year time horizon, although because the O_3 RF changes sign we split it into two components. A time-integrated RF (IRF) is closely related to a Global Warming Potential (GWP), differing only in that it has not been normalized by the IRF from the equivalent mass of CO_2 emission [*Forster et al.*, 2007, p. 210]. The initial increase in O_3 generates a positive RF with a distinct regional structure, related to both the horizontal distribution of the O_3 anomaly (Figure 1a) and the coincident physical properties of the atmosphere and surface (e.g., vertical profiles of temperature and cloud, albedo). Detailed radiative transfer calculations were not performed. Instead, RFs calculated in earlier work (ST04) were normalized to changes in O_3 column, for each month and each 5° × 5° model grid-square. These RFs took stratospheric temperature adjustment into account. Changes in O_3 column from the new experiments were then converted to grid-square RFs using these fields. Using normalized RFs introduces minor errors associated with slight differences in the vertical profile of the O_3 perturbations, but these are insignificant (comparing RFs calculated with the radiative transfer model from ST04 with equivalent RFs calculated from column O_3 changes, we find typical differences of less than 5%). For each month, the global RF is calculated from the individual model grid-square RFs. A global, time-integrated RF is then calculated for each experiment by summing all the months with a positive RF. Figure 2a shows the short-term positive O_3 IRF (units mW m^{-2} yr) for each of the experiments. Each grid-box in Figure 2

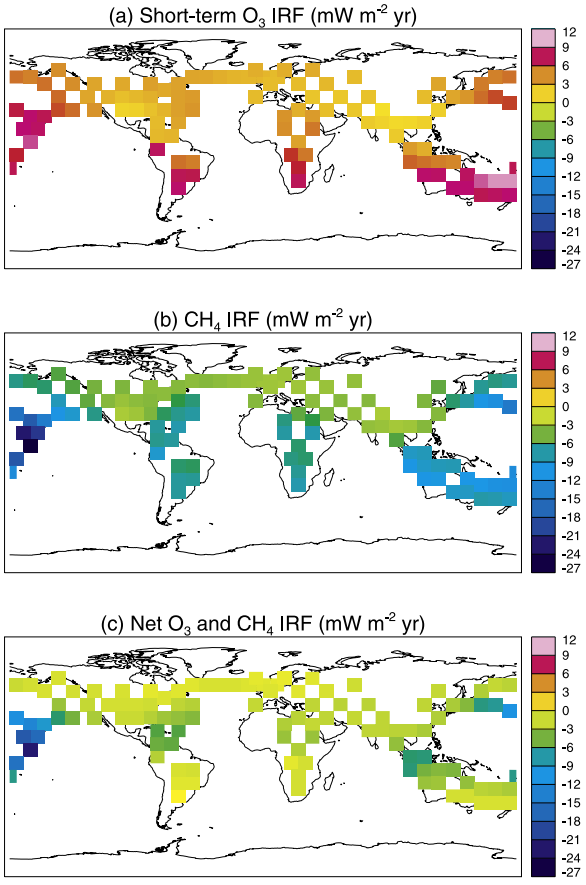

Figure 2. Calculated (stratospheric adjusted) time-integrated radiative forcings (relative to the base) for: (a) the short-term O_3 component; (b) the CH_4 component; and (c) the total net (sum of the short- and long-term O_3 and CH_4 components). Each box shows the global IRF associated with the aircraft emissions from that location. All forcings are normalised to a 1 $Tg(NO_2)$ emission pulse.

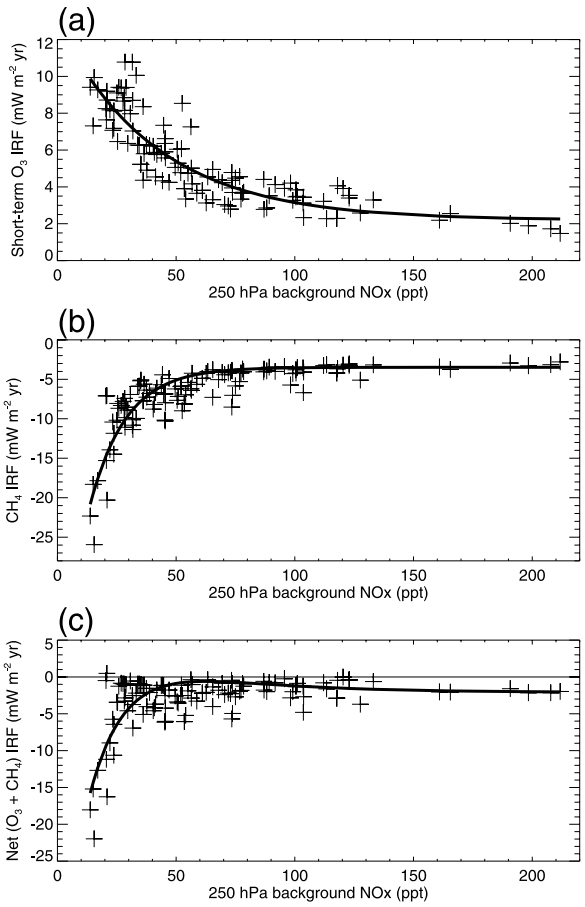

Figure 3. Scatter plots of IRF components ((a) short-term O_3; (b) CH_4; and (c) net) against background NO_x (ppt) at the emission location. Crosses are individual experiments; lines are best-fit curves (see text for details).

represents a global IRF value. The IRFs have been normalized to a pulse of size 1 Tg(NO_2) to make them directly comparable with earlier work; all IRFs quoted here are normalized to this pulse size.

[8] Figure 2b shows CH_4 IRFs. To calculate these, we first extrapolated the CH_4 anomaly (Figure 1c) out to 100 years, using our best estimate of the perturbation e-folding time of 11.5 years (see ST04). Because our experiments are only 1 year long, the CH_4 anomaly has not had sufficient time to become globally well mixed, consequently it shows some month-to-month variability (Figure 1c), and this causes some uncertainty in the initial value to use for the extrapolation. We use the average of the last eight months of each run to represent the peak CH_4 perturbation. We then integrate with respect to time, assume the CH_4 anomaly is globally well-mixed, and convert to an IRF using a value of 0.37 mW m^{-2} ppb^{-1} [*Schimel et al.*, 1996]. There is an additional long-term negative O_3 IRF associated with the negative CH_4 anomaly; this is seen in the negative perturbation to the O_3 burden (Figure 1b). ST04 found that for pulses of aircraft NO_x emissions, followed over 5 years, the ratio between the IRF arising from the long-term O_3 anomaly and the long-term CH_4 anomaly was 0.23, and we apply this simple scaling here to estimate the long-term O_3 IRF components. Figure 2c shows the net IRF arising from both O_3 components and CH_4 for each experiment.

[9] The short-term O_3 IRFs (Figure 2a) are all positive and vary from 1.5 to 11 mW m^{-2} yr over S. Asia and the S. Pacific, respectively. The CH_4 IRFs (Figure 2b) are all negative and vary between −2.8 and −26 mW m^{-2} yr, with smaller magnitudes over Asia, N. America and Europe, and more strongly negative values over the remote Pacific. The net of the O_3 and CH_4 IRFs shows a large amount of cancellation, ranging from −22.0 to 0.5 mW m^{-2} yr, the extremes at locations over the central Pacific and S. America, respectively. It should be noted that these are global average values, and conceal significant regional variation (e.g., the positive O_3 IRF will be exerted more locally, see Figure 1a, but the CH_4 and long-term O_3 IRFs will be exerted more globally), and consequently the climate response may also be quite heterogeneous [cf. *Shindell and Faluvegi*, 2009].

[10] Spatial variations in the IRF magnitudes correlate well with background NO_x at the emission location (Figure 3). The largest magnitude O_3 and CH_4 IRFs tend to be generated from emission sites with low background NO_x, remote from local sources, whilst the lowest magnitude IRFs occur at more polluted locations. Exponential form curves were fit to the data (Figures 3a and 3b); the latitude of emission was also found to be helpful in explaining the O_3 IRF results. The following relationships were found:

$$\mathrm{IRF_{O3}} = 10.7\exp(-0.0242\ \mathrm{bNO_x}) - 0.0165\varphi + 2.57; \quad (1)$$

$$\mathrm{IRF_{CH4}} = -43.0\exp(-0.0656\ \mathrm{bNO_x}) - 3.48; \quad (2)$$

where background NO_x mixing ratios (bNO_x) at the emission sites are in ppt, latitude (φ) is in degrees, and the IRFs have units of mW m^{-2} yr (Tg NO_2)$^{-1}$. Figure 3c shows the net IRF against background NO_x; this curve is simply the sum:

$$\mathrm{IRF_{net}} = \mathrm{IRF_{O3}} + 1.23\ \mathrm{IRF_{CH4}}, \quad (3)$$

which includes the long-term O_3 component (23% of IRF_{CH4}).

[11] It should be noted that these formulae are appropriate for aircraft NO_x emitted in July, and that different results would be found for different months, e.g., see ST04. In particular, the latitude dependence probably mainly stems

Table 1. Global IRFs (mW m^{-2} yr (Tg NO_2)$^{-1}$) From This Study, Calculated Using Equations (1)–(3), With Comparable Values From Earlier Work

Vertical extent and season of pulse, and reference	IRF_{O3}/mW m^{-2} yr (Tg NO_2)$^{-1}$	IRF_{CH4}/mW m^{-2} yr (Tg NO_2)$^{-1}$	IRF_{net}/mW m^{-2} yr (Tg NO_2)$^{-1}$
Cruise altitudes, July, this study	4.1	−4.9	−1.9
All altitudes, July, (ST04)	5.1	−4.4	−0.26
All altitudes, Annual [*Wild et al.*, 2001]	7.9	−4.6	+1.8

Table 2. Regional Breakdown (%) of Aircraft NO_x Emissions at Cruise Altitudes and Resulting IRFs

Region[a]	NO_x emission (%)	IRF_{O3} (%)	IRF_{CH4} (%)	IRF_{net} (%)
1. Trans-Pacific(N)	6.9	10.0	10.0	10.0
2. N. America	31.0	26.9	25.5	22.6
3. Trans-Atlantic	9.2	8.8	7.9	6.2
4. Europe	20.8	14.2	15.4	17.8
5. Asia	16.2	14.1	13.4	12.1
6. Trans-Pacific(C/S)	4.1	8.3	11.3	17.6
7. S. America	3.1	5.1	4.9	4.7
8. Africa & Mid-East	5.6	6.8	5.6	3.0
9. Australasia	3.1	6.0	6.1	6.1

[a]Regions (shown in Figure 1a) are arbitrary and have no policy or other significance.

from the amount of daylight, which will clearly change with season.

[12] Equations (1)–(3), together with the modelled background NO_x at 250 hPa and the aircraft NO_x emission distribution, allow us to construct results equivalent to those reported by ST04 for a July perturbation to aircraft emissions at all locations (Table 1). Ozone and CH_4 IRFs agree to within ~20% between the two studies, and give an indication of the uncertainty associated with using different versions of the same model. In addition there are slight differences in methodology, such as here we only consider emissions at cruise altitude, whereas ST04 considered all altitudes; the curve-fitting also introduces approximations. Clearly, the net IRF is significantly different, mainly because it is the result of near cancellation of larger terms.

[13] Table 2 presents a breakdown by world region (shown in Figure 1a) of both the emissions and resultant IRFs, based on equations (1)–(3). It is clear that the less polluted regions in general make larger contributions to the IRF components, meaning that emissions in these regions produce more important impacts. In this study, the negative IRFs associated with CH_4 and long-term O_3 reduction almost universally exceed the positive IRFs associated with the short-term O_3 increase. This means the more sensitive regions show more negative IRFs, i.e., the NO_x emissions in these regions contribute a larger cooling influence. It should be noted that other studies [e.g., *Wild et al.*, 2001] found that the IRF from the short-term O_3 increase dominates the net IRF (Table 1); clearly there is some model-dependence.

4. Discussion and Conclusions

[14] Our experiments show that the location of aircraft NO_x emissions is important, similar to our results for surface NO_x [*Derwent et al.*, 2008]. A major influence is the background NO_x at the emission site. More polluted sites are less sensitive to the addition of more NO_x; the sensitivities of O_3 production and CH_4 destruction also differ. Latitude of emission is also important. We would expect some seasonality in the latitude dependence, based on our earlier results (ST04), but background NO_x levels appear to be the most important control. Our results reflect the fact that photochemical production of oxidants is non-linearly related to precursor concentrations and UV radiation [*Lin et al.*, 1988; *Isaksen et al.*, 2005]. *Grewe and Stenke* [2008] simulated the effects of aircraft NO_x emissions released at 198 hPa in four latitude bands, and found the O_3 RF varied from 18 mW m^{-2} (Tg NO_2)$^{-1}$ in the tropics to 1.5 mW m^{-2} (Tg NO_2)$^{-1}$ at 60–90°N, similar to our results (Figure 2a).

[15] To put these results in perspective, we can compare them with the associated positive RF (climate warming) from aviation CO_2. If we take the NO_x to CO_2 emission ratio from the NASA 1992 inventory [*Penner et al.*, 1999], then the IRF for CO_2 is 28 mW m^{-2} yr for the 1 Tg NO_2 pulse. As CO_2 is long-lived and well-mixed, this value does not vary with emission location or with season, unlike the NO_x IRF. Locally, the magnitude of the climate cooling from July aircraft NO_x emissions approaches the IRF from CO_2 (see Figure 2c: −22 mW m^{-2} yr over the central Pacific). Elsewhere, the positive IRF from CO_2 generally dominates over the negative net IRF from the July NO_x emissions by a large factor. Whilst we expect some seasonal dependence of our results, we nevertheless expect to find similar results for other months (cf. ST04).

[16] The non-CO_2 climate impacts of global aviation were highlighted by *Penner et al.* [1999] who introduced the concept of radiative forcing index (RFI), which is the ratio of the total RF at a particular time to the RF derived from CO_2 emissions. Some current policy documents (see *Forster et al.* [2006] for examples) use an RFI of ~2.5 as a simple multiplicative factor of CO_2 emissions to estimate the climate impact of aviation. *Forster et al.* [2006] clearly argue that RFI is not an appropriate climate metric for aviation, but that integrated measures of the future effects of an emission, such as IRFs, are much more useful. Net IRFs for aircraft NO_x calculated here show considerable spatial variation (Table 2). The net IRF over the Atlantic is two-thirds of the value expected based on emissions magnitude alone, whilst the net IRF for the central/southern Pacific is over four times larger than expected. Using a single value to express the climate impact of global aviation NO_x emissions (or indeed all non-CO_2 effects [e.g., *Lee et al.*, 2009]) therefore conceals considerable spatial variation. The near-cancellation found here between the IRF terms for aviation NO_x also appears to be model-dependent. Consequently further calculations, across a range of models, of the geographical variations in the non-CO_2 climate impacts of global aviation are urgently required to increase our confidence in these results, and to enable such results to be translated into useful policies.

[17] **Acknowledgments.** The development and application of the STOCHEM model was supported by the UK Defra through contract AQ0902 Scientific Support for National and International Policy. DSS thanks NERC for support from grant NE/D012538/1.

References

Dentener, F., D. Stevenson, J. Cofala, R. Mechler, M. Amann, P. Bergamaschi, F. Raes, and R. Derwent (2005), The impact of air pollutant and methane emission controls on tropospheric ozone and radiative forcing: CTM calculations for the period 1990–2030, *Atmos. Chem. Phys.*, *5*, 1731–1755.

Derwent, R. G., W. J. Collins, C. E. Johnson, and D. S. Stevenson (2001), Transient behaviour of tropospheric ozone precursors in a global 3-D CTM and their indirect greenhouse effects, *Clim. Change*, *49*, 463–487, doi:10.1023/A:1010648913655.

Derwent, R. G., D. S. Stevenson, R. M. Doherty, W. J. Collins, M. G. Sanderson, and C. E. Johnson (2008), Radiative forcing from surface NO_x emissions: Spatial and seasonal variations, *Clim. Change*, *88*, 385–401, doi:10.1007/s10584-007-9383-8.

Forster, P. M. F., K. P. Shine, and N. Stuber (2006), It is premature to include non-CO_2 effects of aviation in emission trading schemes, *Atmos. Environ.*, *40*, 1117–1121, doi:10.1016/j.atmosenv.2005.11.005.

Forster, P., et al. (2007), Changes in atmospheric constituents and in radiative forcing, in *Climate Change 2007: The Physical Science Basis. Contribution of Working Group I to the Fourth Assessment Report of the Intergovernmental Panel on Climate Change*, edited by S. Solomon et al., pp. 129–234, Cambridge Univ. Press, New York.

Grewe, V., and A. Stenke (2008), AirClim: An efficient tool for climate evaluation of aircraft technology, *Atmos. Chem. Phys.*, *8*, 4621–4639.

Isaksen, I. S. A., C. Zerefos, K. Kourtadis, C. Meleti, S. B. Dalsøren, J. K. Sundet, A. Grini, P. Zanis, and D. Balis (2005), Tropospheric ozone changes at unpolluted and semi-polluted regions induced by stratospheric ozone changes, *J. Geophys. Res.*, *110*, D02302, doi:10.1029/2004JD004618.

Köhler, M. O., G. Radel, O. Dessens, K. P. Shine, H. L. Rodgers, O. Wild, and J. A. Pyle (2008), Impact of perturbations to nitrogen oxide emissions from global aviation, *J. Geophys. Res.*, *113*, D11305, doi:10.1029/2007JD009140.

Lee, D. S., D. W. Fahey, P. M. Forster, P. J. Newton, R. C. N. Wit, L. L. Lim, B. Owen, and R. Sausen (2009), Aviation and global climate change in the 21st century, *Atmos. Environ.*, *43*, 3520–3537, doi:10.1016/j.atmosenv.2009.04.024.

Lin, X., M. Trainer, and S. C. Liu (1988), On the nonlinearity of the tropospheric ozone production, *J. Geophys. Res.*, *93*, 15,879–15,888, doi:10.1029/JD093iD12p15879.

Penner, J. E., D. H. Lister, D. J. Griggs, D. J. Dokken, and M. McFarland (1999), *IPCC Special Report on Aviation and the Global Atmosphere*, Cambridge Univ. Press, New York.

Schimel, D., et al. (1996), Radiative forcing of climate change, in *Climate Change 1995: The Science of Climate Change*, edited by J. T. Houghton et al., pp. 65–132, Cambridge Univ. Press, New York.

Schumann, U. (2005), Formation, properties and climatic effects of contrails, *C. R. Phys.*, *6*, 549–565, doi:10.1016/j.crhy.2005.05.002.

Shindell, D. T., and G. Faluvegi (2009), Climate response to regional radiative forcing during the 20th century, *Nat. Geosci.*, *2*, 294–300, doi:10.1038/ngeo473.

Stevenson, D. S., R. M. Doherty, M. G. Sanderson, W. J. Collins, C. E. Johnson, and R. G. Derwent (2004), Radiative forcing from aircraft NO_x emissions: Mechanisms and seasonal dependence, *J. Geophys. Res.*, *109*, D17307, doi:10.1029/2004JD004759.

Stevenson, D. S., et al. (2006), Multi-model ensemble simulations of present-day and near-future tropospheric ozone, *J. Geophys. Res.*, *111*, D08301, doi:10.1029/2005JD006338.

Stordal, F., G. Myhre, E. J. G. Stordal, W. B. Rossow, D. S. Lee, D. W. Arlander, and T. Svendby (2005), Is there a trend in cirrus cloud due to aircraft traffic?, *Atmos. Chem. Phys.*, *5*, 2155–2162.

Wild, O., M. J. Prather, and H. Akimoto (2001), Indirect long-term global radiative cooling from NO_x emissions, *Geophys. Res. Lett.*, *28*, 1719–1722, doi:10.1029/2000GL012573.

R. G. Derwent, rdscientific, Newbury RG14 6LH, UK. (r.derwent@btopenworld.com)

D. S. Stevenson, School of GeoSciences, University of Edinburgh, King's Buildings, Edinburgh EH9 3JN, UK. (dstevens@staffmail.ed.ac.uk)